OPEN

Citation: Oncogenesis (2013) **2**, e68; doi:10.1038/oncsis.2013.33

www.nature.com/oncsis

ORIGINAL ARTICLE

A novel orthotopic mouse model of head and neck cancer and lymph node metastasis

R Masood[1], C Hochstim[1], B Cervenka[1], S Zu[1], SK Baniwal[2], V Patel[3], A Kobielak[1] and UK Sinha[1]

Prognosis of head and neck squamous cell carcinoma (HNSCC) is largely determined by the extent of lymph node (LN) metastasis at diagnosis, and this appears to be controlled by cancer cell genetics. To examine the role of these genes in LN metastasis, we created a human-in-mouse orthotopic model of HNSCC and performed comparative microarray analysis of gene expression between populations of HNSCC cell lines derived before and after serial transplantation and *in vivo* metastasis in mice. Microarray analysis comparing the USC-HN3-GFP, USC-HN3-GFP-G1 and USC-HN3-GFP-G2 cell lines identified overexpression of genes implicated in epithelial-to- mesenchymal transition and the formation of cancer stem cells, including *CAV-1*, *TLR-4* (Toll-like receptor 4), *MMP-7* (matrix metalloproteinase 7), *ALDH1A3*, *OCT-4* and *TRIM-29*. Ingenuity Pathway Analysis confirmed upregulation of respective gene signaling pathways in the USC-HN1-GFP-G2 cell line. Patient HNSCC samples from advanced stages overexpressed *ALDH1A3*, *CAV-1* and *MMP-7*. Our results show that *CAV-1*, *TLR-4*, *MMP-7*, *ALDH1A3*, *OCT-4* and *TRIM-29* have increased expression in HNSCC cells selected for an enhanced metastatic phenotype and suggest that these genes may have an important role in the metastatic potential of HNSCC cells. Inhibition of these genes may therefore have prognostic and therapeutic utility in HNSCC.

Oncogenesis (2013) **2,** e68; doi:10.1038/oncsis.2013.33; published online 9 September 2013

Subject Categories: cell cycle and growth regulation

Keywords: head and neck squamous cell carcinoma genetics; metastasis; epithelial-to-mesenchymal transition (EMT); cancer stem cells (CSCs)

INTRODUCTION

Head and neck squamous cell carcinoma (HNSCC) is the sixth most common cancer worldwide.[1] In 2010, it accounted for 49 260 new cancer diagnoses and 11 480 deaths in the United States.[1] Prognosis of HNSCC is largely determined by the extent of lymphatic invasion and metastasis at diagnosis. Nearly 50% of patients with HNSCC have lymphatic metastasis, which accounts for the persistently poor prognosis over the past several decades despite advancement in our understanding of prevention and treatment.[1]

Risk factors for HNSCC can be subdivided into three groups: chronic irritants of the upper aerodigestive tract, human papillomavirus induced alterations of the cell cycle, and genetic syndromes characterized by DNA-repair defects and genomic instability. Tobacco, alcohol and betel nut use are chronic irritants. Tobacco alone increases the risk 3–9-fold, and when exposed in combination with alcohol carries a synergistic risk of approximately 100-fold.[2] It has recently been shown that HNSCC in tobacco users have more gene mutations than in non-tobacco users, and these genes been demonstrated to be essential for tumor growth.[3,4] Human papillomavirus, through manipulation of the cell cycle, has been demonstrated to increase the risk of a specific subset of HNSCC that occurs primarily in the hypopharynx.[5] This subset has been recently demonstrated to have fewer gene mutations than HNSCC not associated with human papillomavirus.[3,4]

In HNSCC, the ability to invade the lymphatic system is not determined by the size of the primary tumor, rather it is an intrinsic characteristic of the tumor itself. There have been numerous studies demonstrating differences between gene expression profiles of primary and metastatic HNSCC, suggesting that specific gene alterations drive the molecular processes responsible for metastasis.[6] This molecular understanding has translated to targeted therapy. Epidermal growth factor receptor (EGFR) was identified as a key upregulated protein receptor in metastatic HNSCC and led to the development of an EGFR-blocking antibody, cetuximab. This has demonstrated improved survival when combined with chemotherapy alone or radiotherapy alone.[7] Our understanding of the specific genetic changes underlying metastatic disease and our ability to generate targeted therapies is still limited.

The epithelial-to-mesenchymal transition (EMT) describes a process by which a polarized epithelial cell develops a mesenchymal phenotype, decreased E-cadherin expression and increased vimentin expression.[8] This has been associated with increased invasiveness, metastasis, recurrence and a poor clinical prognosis.[8] EMT has been demonstrated to be associated with changes in specific gene expression.[9] Cancer stem cells (CSCs) are a group of highly tumorigenic cells that have the ability to self-renew and produce differentiated heterogeneous progeny. They have been identified in a variety of solid and hematological cancer types using cancer-specific cell markers. CSCs are relevant to tumor biology because of their major role in recurrence and metastasis.[10] There have been specific gene expression changes associated with the formation of CSCs.[11]

[1]Department of Otolaryngology–Head and Neck Surgery, Keck School of Medicine, University of Southern California, Los Angeles, CA, USA; [2]Department of Orthopaedic Surgery, Keck School of Medicine, University of Southern California, Los Angeles, CA, USA and [3]Oral and Pharyngeal Cancer Branch, National Institute of Dental and Craniofacial Research, National Institute of Health, Bethesda, MD, USA. Correspondence: Dr R Masood, Department of Otolaryngology–Head and Neck Surgery, Keck School of Medicine, University of Southern California, HMP-903, 2011 Zonal Avenue, Los Angeles, CA 90033, USA.
E-mail: masood@usc.edu
Received 8 July 2013; accepted 29 July 2013

Murine models were first used as platforms to analyze systemic drug effects in cancer.[12] The first murine xenograft models injected human HNSCC subcutaneously, but it was soon discovered that preclinical results from these models did not translate to clinical trials because the location failed to recapitulate organ-specific environments that would support locoregionally invasive or metastatic disease.[12] Orthotopic murine models utilized the tongue for placement of SCC and have demonstrated the successful development of primary tumors histologically similar to oral tongue SCC with metastasis following the expected cervical lymph node (LN) pattern.[12,13] These models have been utilized to perform *in vivo* selection for highly metastatic HNSCC cell lines and are therefore ideal for the *in vivo* study of the genetic changes responsible for metastasis.[6]

In this study, we developed an orthotopic murine model of HNSCC using the USC HN3-GFP HNSCC cell line injected into the tongues of SCID/nude mice. Metastatic cell isolation was enhanced by fluorescence-activated cell sorter (FACS) utilizing the green fluorescent protein (GFP), allowing selection for a pure, immortal metastatic cell line. The resulting USC-HN3-GFP-G2 cell line demonstrated more aggressive metastatic behavior and phenotypic and gene expression changes consistent with EMT. Using microarray analysis, western blotting and immunohistochemistry (IHC), we characterized changes in gene and protein expression associated with the enhanced metastatic phenotype, including *CAV-1*, *TLR-4* (Toll-like receptor 4), *MMP-7* (matrix metalloproteinase 7), *TRIM-29*, *ALDH1A3* and *OCT-4*. Genes identified in the metastatic model were also overexpressed in patient HNSCC tumor and LN samples as demonstrated by western blotting and IHC. These genes include *ALDH1A3*, *CAV-1* and *MMP-7*.

RESULTS

A mouse xenograft model of HNSCC: a platform for therapeutic studies

The stably transfected USC-HN3-GFP cells were selected by using FAC,S and the pure USC-HN3-GFP cells were isolated and grown in 10% of DMEM (Dulbecco's modified Eagle's medium). Around 2.5 million stably transfected USC-HN1-GFP cells were injected into the tongues of six SCID/nude mice. At day 28, the mice were killed, and images of the tongue and tumor tissue were captured using fluorescent microscopy (Figure 1a). All six mice demonstrated primary tumors of the tongue and metastasis to cervical LNs. Skin and muscle were removed from the neck, and green-fluorescing cells were identified in their migration from the primary tumor to the LN in the neck. Fluorescent microscopy was used to identify metastatic GFP-transfected tumor cells. Metastatic tumor cells from LNs containing fluorescent tumor were harvested.

The green-fluorescing cells that we isolated from the LN of the mice were then analyzed using hematoxylin and eosin staining and IHC and demonstrated increased expression of EGFR and Ki-67 as demonstrated in (Figure 1b). To purify and expand the resultant cell line, the isolated cells from the neck metastasis were

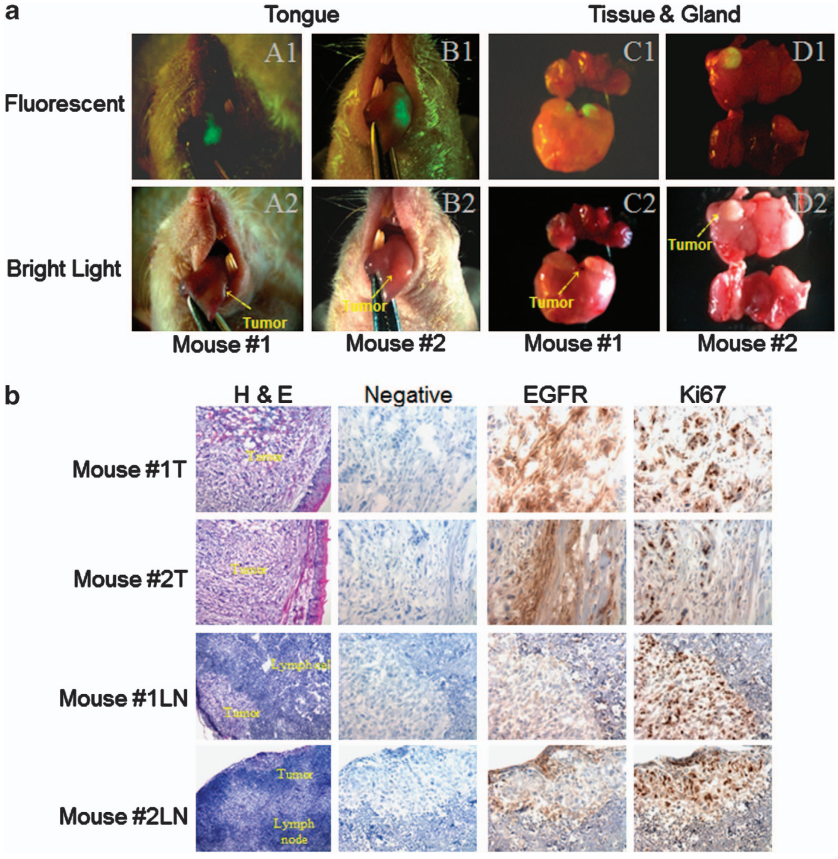

Figure 1. Establishment of the USC-HN3-GFP HNSCC cell line in the xenograft mouse model. (**a**) Primary tumor growth of USC-HN3-GFP cells in two representative xenograft mice after 4 weeks of growth under fluorescent and bright light microscopy. Flourescent microscopy demonstrated tumor in the tongue (A1, B1) and tumor in the tissue and gland (C1, D1). Bright light microscopy demonstrated tumor in the tongue (A2, B2) and tumor in the tissue and gland (C2, D2). (**b**) Hematoxylin and eosin staining and IHC of the primary tumor and LN metastasis tissue in the mouse model. Tissue is stained with antibodies against EGFR and Ki-67. Primary tumor and LN demonstrate histological features consistent with SCC. Expression of EGFR and Ki-67 indicates that primary tumor and LN are neoplastic cells with high proliferative index. Negative control was stained without primary antibody.

purified using FACS and expanded in culture to develop an immortal cell line, USC-HN3-GFP-G1. We then injected the USC-HN3-GFP-G1 cell line into the tongues of six SCID/nude mice and this led to earlier and more extensive tumor development, as seen in (Figure 2a). All six mice demonstrated primary tumors and cervical LN involvement. In all, 83% demonstrated lung metastasis and 67% demonstrated liver metastasis. We again used fluorescent microscopy to isolate green-fluorescing metastatic USC-HN3-GFP-G1 cells from the LN and cultured and expanded the cells developing the immortal USC-HN3-GFP-G2 cell line. Cell migration assays were conducted to compare migration behavior of the cell lines. Double chamber cellular migration assay (data not shown) utilizing fetal bovine serum (FBS) demonstrated increased migration in the USC-HN3-GFP-G1 and USC-HN3-GFP-G2 cell lines when compared with the parent USC-HN3-GFP cell line.

Highly metastatic USC-HN3-GFP-G2 cell line demonstrates phenotypic and surface protein expression changes consistent with EMT

To test our hypothesis that the highly metastatic cells generated from the LNs had undergone EMT, we first expanded the immortal USC-HN3-GFP-G2 cell line and then performed five passages of trypsinization and expansion to isolate the pure population of tumor cells. When we compared the resultant cells under bright light and fluorescent microscopy, an increasingly spindle morphology consistent with mesenchymal cells was seen (Figure 2b). We then performed immunofluorescence and demonstrated a progressive cell surface downregulation of E-cadherin and co-localized protein, β-catenin, in the USC-HN3-GFP-G1 and USC-HN3-GFP-G2 cell lines compared with the parental USC-HN3-GFP generation (Figure 2c).

Microarray analysis, western blotting and IHC identifies overexpression of CSC- and EMT-associated genes in highly metastatic USC-HN3-GFP-G1 and USC-HN3-GFP-G2 cell lines

A global expression profile was carried out using Illumina BeadChip Human HT-12 v4 expression arrays in the following three cell lines: USC-HN3-GFP, USC-HN3-GFP-G1, and USC-HN3-GFP-G2. Genes were identified that demonstrated increased expression in the highly metastatic generation of cells (Table 1). We found that several key genes in CSC formation were overexpressed in the USC-HN3-GFP-G2 cell line, including *ALDH1A3*, *OCT-4* and *ABCG2* (Table 1). This pattern was also observed in EMT- and CSC-associated genes, including *CAV-1*, *TLR-4*, *TRIM-29* and *MMP-7* (Table 1). Western blotting demonstrated increased protein expression of the *OCT-4*, *ALDH1A3*,

Table 1. Gene expression changes and *P*-values of USC-HN3-GFP, USC-HN3-GFP-G1 and USC-HN3-GFP-G2 cell lines

USC-HN3 cell lines	*USC-HN3-GFP-G1*		*USC-HN3-GFP-G2*	
	Fold change	P-*value*	*Fold change*	P-*value*
CSC biomarkers				
ALDH1A3	2.31	0.02	>3	0.000472
OCT-4	−1.73	0.4	1.93	0.01
Associated genes				
TLR-4	1.7	0.88	2.5	0.000187
CAV-1	1.93	0.05	2.61	0.000145
TRIM-29	2.35	0.004	>3	0.00991
MMP-7	1.75	0.75	>3	0.00028

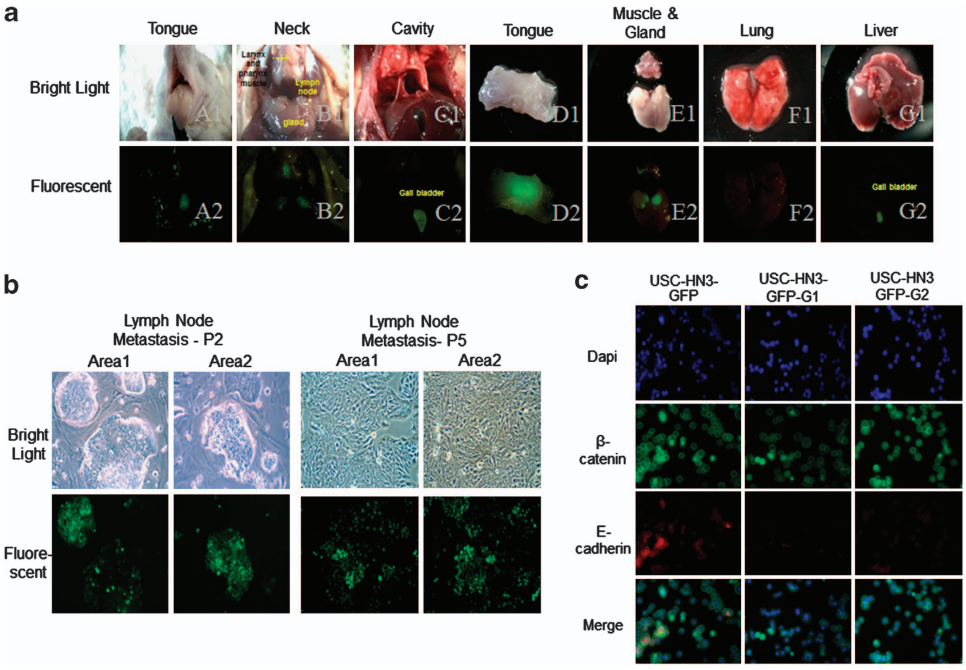

Figure 2. USC-HN3-GFP-G1 cell line highly metastatic and the resultant USC-HN3-GFP-G2 cell line demonstrating changes consistent with EMT. (**a**) Fluorescent and bright light microscopy of representative xenograft mouse demonstrating primary tumor of the tongue (A1, A2), local invasion of the neck (B1, B2) and regional metastasis in gallbladder (C1, C2) of the USC-HN3-GFP-G1 cell line after 4 weeks. The respective organs were dissected and pictures were taken on bright light and fluorescent imaging as shown in the lower panels. Tongue (D1, D2), muscle and gland (E1, E2), lung (F1, F2) and liver (G1, G2). (**b**) Bright light and fluorescent microscopy demonstrating purified metastatic USC-HN3-GFP-G2 cell line from LN in culture developing increasingly spindle-shaped morphology consistent with EMT. P2 and P5 indicate passages of cell culture. (**c**) Immunofluorescence demonstrating progressive downregulation of surface β-catenin and E-cadherin in the USC-HN3-GFP-G1 and USC-HN3-GFP-G2 cell lines compared with the USC-HN3-GFP cell line. The merge pictures of β-catenin and E-cadherin are shown in the lower panels. DAPI, 4,6-diamidino-2-phenylindole.

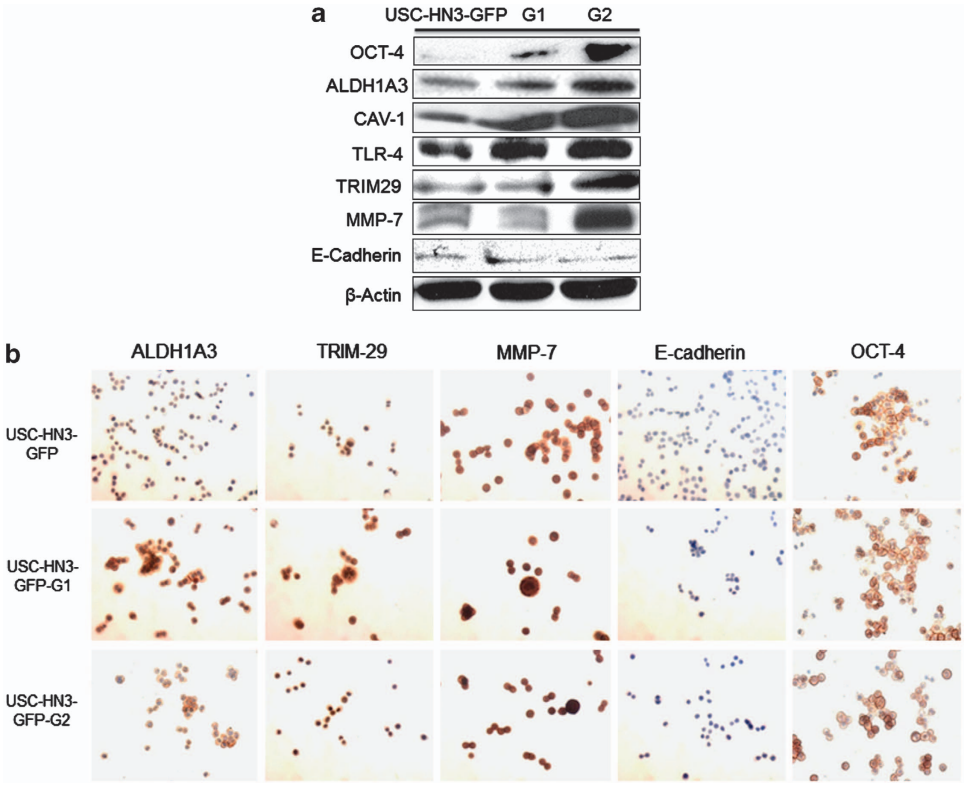

Figure 3. Western blotting and IHC of the USC-HN3-GFP, USC-HN3-GFP-G1 and USC-HN3-GFP-G2 cell lines. (**a**) Western blot demonstrating progressively increasing expression of *OCT-4*, *ALDH1A3*, *CAV-1*, *TLR-4*, *TRIM-29* and *MMP-7* in the metastatic USC-HN3-GFP-G1 and USC-HN3-GFP-G2 cell lines. E-cadherin expression is progressively decreasing in the metastatic USC-HN3-GFP-G1 and USC-HN3-GFP-G2 cell lines as compared with the USC-HN3-GFP cell line. (**b**) Immunocytochemistry ($\times$ 20) of USC-HN3-GFP, USC-HN3-GFP-G1 and USC-HN3-GFP-G2 cell lines demonstrating increasing expression of *ALDH1A3*, *TRIM-29*, *MMP-7* and *OCT-4*. E-cadherin expression is progressively decreasing in the metastatic USC-HN3-GFP-G1 and USC-HN3-GFP-G2 cell lines.

CAV-1, *TLR-4*, *TRIM-29* and *MMP-7* genes and decreasing expression of E-cadherin in the USC-HN3-GFP-G1 and USC-HN3-GFP-G2 cell lines when compared with USC-HN3-GFP (Figure 3a). IHC on the cell lines demonstrated increasing expression of the *ALDH1A3*, *TRIM-29*, *MMP-7* and *OCT-4* gene products in the USC-HN3-GFP-G1 and USC-HN3-GFP-G2 cell lines and a decreasing E-cadherin protein expression in the USC-HN3-GFP-G1 and USC-HN3-GFP-G2 cell line (Figure 3b).

Ingenuity Pathway Analysis (IPA) demonstrates upregulation of key tumorigenic pathways and CSC-and EMT-associated gene networks.

We used IPA to compare functional networks and key gene signaling pathways between the USC-HN3-GFP, USC-HN3-GFP-G1 and USC-HN3-GFP-G2 cell lines. There was progressive upregulation of functional gene networks associated with 'cell growth and proliferation', 'tumor morphology', 'cellular development', 'cell death and survival', 'cell movement and cell morphology' in the metastatic USC-HN3-GFP-G1 and USC-HN3-GFP-G2 cell lines (Figure 4b). There was upregulation of genes in the signaling networks of *ALDH1A3*, *OCT-4*, *TRIM-29*, *MMP-7*, *CAV-1* and *TLR-4* in the USC-HN3-GFP-G2 cell line (Figure 4a).

Patient HNSCC tissues demonstrate gene expression changes observed in mouse xenograft model

Using the metastatic xenograft model, we identified genes that are overexpressed in association with metastasis. We then performed a functional analysis to identify whether these genes are also upregulated in human HNSCC. We prepared tissue sections from eight HNSCC samples, all coming from patients with advanced stage HNSCC, and performed western blotting and IHC. We found similar protein overexpression of the following genes, *TRIM-29*, *ALDH1A3*, *OCT-4*, *CAV-1*, *MMP-7* and *β-catenin* in the tumor tissues and/or LN tissues (Figures 5a–d).

DISCUSSION

HNSCC is the sixth most common cancer worldwide.[1] Prognosis in HNSCC is largely determined by the extent of lymphatic invasion and metastasis when diagnosed. Nearly 50% of patients with HNSCC have lymphatic metastasis, which accounts for the persistently poor prognosis over the past three decades.[15] The specific genetic alterations leading to an enhanced ability of HNSCC to metastasize is an area of intense research, as these genes serve as ideal targets for molecular interventions.

Orthotopic murine models are ideal for identifying genetic changes involved in metastasis, because they allow for the repetitive collection of metastatic cells from LNs and reimplantation of these cells to create *in vivo* selection for a highly metastatic cell lines. These cells, when compared with the parental generation, highlight key gene alterations associated with metastasis. A number of murine models have been developed by several investigators and have demonstrated changes in gene expression correlated with metastasis.[6,16] Our model used a similar xenograft murine model platform but took advantage of GFP, fluorescent microscopy and FACS to isolate a highly purified metastatic cell line. This circumvents aberrant gene expression changes secondary to impure tumor samples.

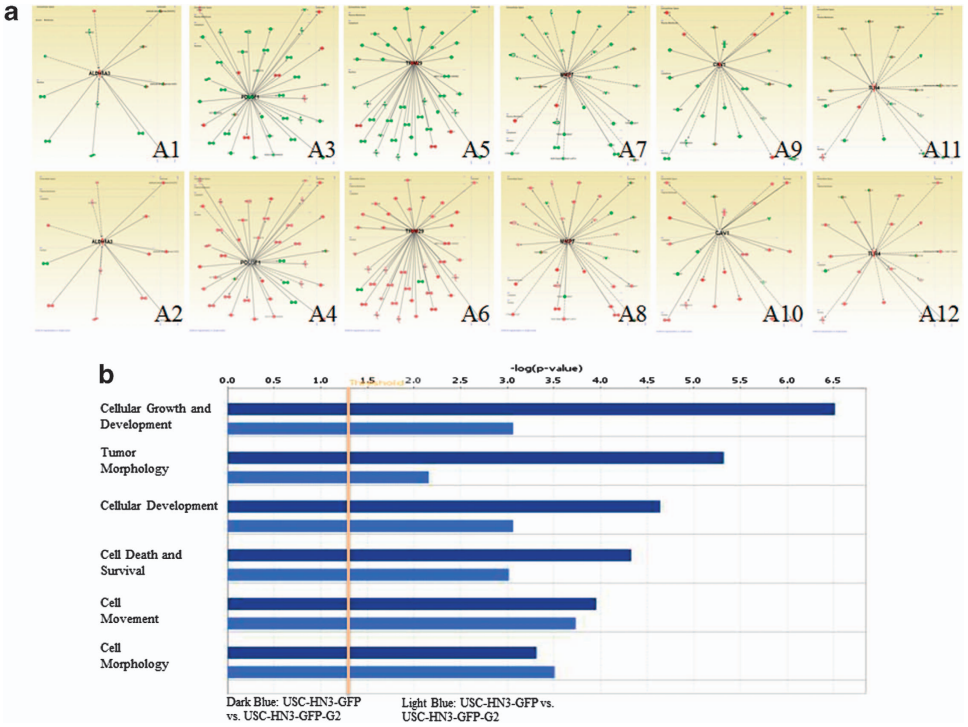

Figure 4. IPA analysis of functional gene networks and signaling pathways. (**a**) Core analysis of the signaling pathways in the USC-HN3-GFP and USC-HN3-GFP-G2 cell lines. Green indicates under expression and red overexpression. The majority of the following gene networks were overexpressed in the USC-HN3-GFP-G2 cell line as compared with the USC-HN3-GFP-G1 cell lines: *ALDH1A3* (A1, A2), *OCT-4* (A3, A4), *TRIM-29* (A5, A6), *MMP-7* (A7, A8), *CAV-1* (A9, A10), and *TLR-4* (A11, A12). (**b**) IPA core analysis of functional networks demonstrating progressive upregulation of 'cellular growth and proliferation genes', 'tumor morphology genes', 'cellular development genes', 'cell death and survival genes' and 'cell movement genes' in the USC-HN3-GFP-G1 and USC-HN3-GFP-G2 cell lines as compared with parental USC-HN3-GFP cell line. 'Cell morphology genes' were overexpressed in both the cell lines, but there was less overexpression in the USC-HN3-GFP-G2 cell line as compared with USC-HN3-GFP-G1 cell line. Light blue indicates USC-HN3-GFP-G1 vs USC-HN3-GFP functional network gene expression values, and dark blue indicates the USC-HN3-GFP-G2 vs USC-HN3-GFP functional network gene expression values.

EMT describes a process by which a polarized epithelial cell develops a mesenchymal phenotype, loss of cell polarity, decreased E-cadherin cell surface expression and subsequently demonstrate increased motility and invasiveness.[8] It has been demonstrated that acquisition of this mesenchymal phenotype correlates with recurrence, metastasis and a poor clinical prognosis.[10] Our highly metastatic USC-HN3-GFP-G2 cell line acquired a spindle morphology, demonstrated a cell surface downregulation of E-cadherin and co-localized β-catenin and increased *in vitro* migration, all consistent with EMT.[6] Additionally, microarray analysis and IPA demonstrated overexpression of a significant number of genes associated with EMT in the highly metastatic USC-HN3-GFP-G2 cell line, notably *HIF-1α*, *EDN-1* and *β-catenin*.[6,10,17]

CSCs are a group of highly tumorigenic cells that have the ability to self-renew and produce differentiated heterogeneous progeny. They have been identified in a variety of solid and hematological cancer types using cancer-specific cell markers.[10] CSCs have a major role in recurrence and metastasis in a variety of tumors, including HNSCC.[10] In our study, microarray analysis demonstrated overexpression of genes associated with CSCs in the highly metastatic USC-HN3-GFP-G2 cell line, including *OCT-4* and *ALDH1A3*. Additionally, IPA demonstrated overexpression of many of the genes in the *OCT-4* and *ALDH1A3* signaling pathways in the USC-HN3-GFP-G2 cell line.

OCT-4 is a member of the POU domain transcription factors and regulates proliferation and differentiation of embryonic stem cells, germ cells and somatic stem cells.[18] In HNSCC, *OCT-4* has been associated with CSC formation and EMT.[18,19] Recently, in cell culture, it was demonstrated that when *OCT-4* is silenced there is a decrease in the CSC properties and tumorigenic potential of the cell line.[19]

ALDH1 describes a group of isoenzymes whose activity is associated with CSCs in many cancer types, including HNSCC.[20] ALDH1 induction of CSCs may be related to oxidation of retinal to retinoic acid, which is important in the early steps of differentiation in stem cells.[11] The isoenzyme ALDH1A1 is most commonly described as responsible for ALDH1 activity, as measured by the Aldefluor assay, in CSCs.[20] In contrast, we found that *ALDH1A3* was the only ALDH1 isoenzymegene significantly overexpressed in the USC-HN3-GFP-G2 cell line, suggesting that it is the predominant ALDH1 isoenzyme responsible for metastasis and CSC formation in HNSCC. In a melanoma cell line, *ALDH1A3* was the predominant form in an ALDH+ cell line and silencing it led to decreased viability and increased apoptosis *in vitro* and reduced tumorigenesis and chemoresistance *in vivo*.[21] *ALDH1A3* was also described as the predominant form in breast cancer, and this was accounted for by the natural tissue distribution of the isoenzyme.[20] *ALDH1A3* is expressed in the kidneys, stomach, breast, fetal nasal mucosa and salivary glands, whereas *ALDH1A1* is expressed in hematopoietic stem cells, testes, eye, brain, kidney, liver and neural stem cells.[20]

We demonstrated the overexpression of several EMT- and CSC-associated genes in the USC-HN3-GFP-G2 generation, suggesting an association with metastasis and potential targets for molecular inhibitors. These genes include T*RIM-29*, *CAV-1*, *TLR-4* and *MMP-7*. *TRIM-29* has been demonstrated in many cancers, including melanoma, multiple myeloma, endometrial, ovarian and colorectal cancer.[22] *TRIM-29* expression has been correlated with tumor progression and metastasis in gastric carcinoma, non-small cell

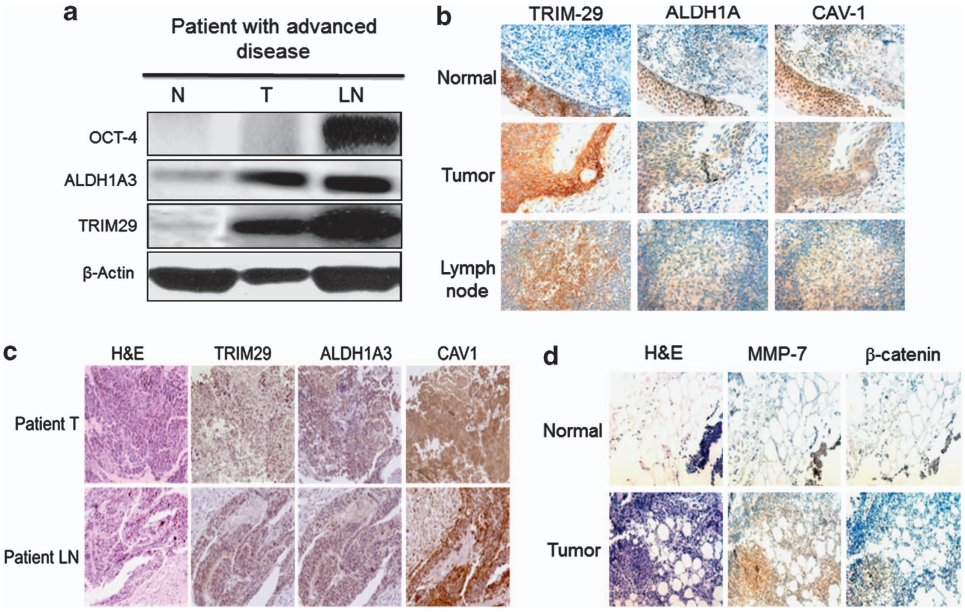

Figure 5. Western blotting and IHC analysis of advanced stage patient HNSCC samples. (**a**) Western blotting demonstrating overexpression of *OCT-4*, *ALDH1A3* and *TRIM-29* in the patient tumor (T) and LN as compared with normal (N) tissue. (**b**, **c**) IHC analysis of an advanced stage HNSCC sample of a patient demonstrating increasing expression of *TRIM-29*, *ALDH1A3* and *CAV-1* in the tumor and LNs as compared with normal tissue. (**d**) IHC analysis of an advanced stage HNSCC sample of a patient demonstrating increasing expression of *MMP-7* and *β-catenin* in the tumor as compared with normal tissue.

lung carcinoma and pancreatic adenocarcinoma.[22,23] To our knowledge, this is the first time that *TRIM-29* has been demonstrated to be upregulated in HNSCC. *TRIM-29* was overexpressed in the highly metastatic USC-HN3-GFP-G2 generation and patient HNSCC samples, suggesting a role in metastasis. In non-small cell lung carcinoma and pancreatic adenocarcinoma, this was secondary to *TRIM-29*-induced *β-catenin* expression and subsequent EMT, which is a possible mechanism in HNSCC.[22,23]

CAV-1 is a cell membrane structural protein that has been demonstrated to have an important role in signal transduction, vesicular transport and cell receptor localization.[24] *CAV-1* expression has been correlated with metastasis and a poor prognosis in many cancer types.[24] In HNSCC, *CAV-1* is progressively upregulated from pre-neoplastic to neoplastic HNSCC.[24,25] Recently, a RNAi lentivirus suppressor of *CAV-1* decreased tumor survivability and increased apoptosis in HNSCC.[26] The function of *CAV-1*in tumorigenesis may be related to its ability to control cell-surface expression of key proteins, such as E-cadherin and β-catenin. It has been shown that *EGFR*-induced *CAV-1* overexpression leads to the internalization of the adherens junction protein, E-cadherin, loss of cell–cell contact and Wnt GSK-3beta-independent EMT signaling.[27] Additionally, *CAV-1* may have an important role in EMT and CSC formation through the enhancement of pro-tumorigenic inflammatory signaling. Walton *et al.*[28] demonstrated that *CAV-1* upregulation enhanced lipopolysaccharide-induced interleukin-8 signaling through TLR-4 in endothelial cells. Here, we demonstrated that *CAV-1* may have an important role in metastasis in HNSCC.

TLR-4 is part of the interleukin-1R receptor family that is expressed classically on antigen-presenting cells but is also seen on other types of immune cells, endothelial cells and epithelial cells.[29] Expression of the *TLR-4* gene has been associated with cancer progression and metastasis in prostate, colon, hepatocellular carcinoma and HNSCC.[29,30] *TLR-4* expression has been associated with the induction of CSCs and EMT in hepatocellular and colon carcinoma.[30,31] In HNSCC, increasing expression of *TLR-4* has been associated with disease progression and metastasis.[29] In HNSCC cell lines, addition of a TLR-4 agonist, lipopolysaccharide, led to cell proliferation and production of interleukin-8, an inducer of EMT and CSC.[29,32,33]

MMP are a family of zinc-dependent enzymes that degrade components of the extracellular matrix and basolateral membrane.[34] MMP-7 (matrilysin) is the smallest of the protein family but is highly active against various extracellular matrices and basement membrane components, including E-Cadherin, type 4 collagen, fibronectin and proteoglycans. *MMP-7* gene expression has been associated with increased disease progression, metastasis and poor overall survival in a variety of epithelial and mesenchymal cancers, including HNSCC.[35] The role of *MMP-7* expression in cancer progression and metastasis is thought to involve the degradation of cell–cell E-cadherin adhesions and the induction of EMT.[36] Shibata *et al.*[36] using an SCC cell line, demonstrated that increasing levels of MMP-7 decreased cell membrane-associated E-cadherin and increased soluble fragments in the medium.

In conclusion, we have successfully developed a xenograft metastatic murine model for HNSCC using GFP-labeled cells and FACS for generation of a pure metastatic cell line. We identified a number of genes, including *CAV-1*, *TLR-4*, *MMP-7*, *TRIM-29*, *ALDH1A3* and *OCT-4*, that may have an important role in metastasis in HNSCC, possibly through the induction of EMT and formation of CSCs. These genes are therefore ideal targets for molecular inhibitors. The molecular inhibitors to these genes are currently being developed, and this xenograft model will serve as an ideal platform testing of these inhibitors in a controlled, reproducible setting.

MATERIALS AND METHODS

Materials

The following antibodies were used: TLR-4, MMP-7, β-catenin, EGFR, and E-cadherin monoclonal antibodies were procured from Santa Cruz Biotechnology, Santa Cruz, CA, USA; OCT-4 and TRIM-29 polyclonal antibodies from Abcam, Cambridge, MA, USA; CAV-1 polyclonal antibody from Transductional Lab BD, San Jose, CA, USA; ALDH1A3 rabbit polyclonal

antibody from ThermoScientific, Rockford, IL, USA; and β-actin monoclonal anti-β-actin antibody clone AC-15 from Sigma-Aldrich, St Louis, MO, USA.

Establishment and development of a unique HNSCC cell line designated USC-HN3 and development of immortal cell line, USC-HN3-GFP

We recently developed the USC-HN3 cell line using methods as described in a previous study.[14] This cell line was derived from an invasive primary right superior alveolar ridge squamous cell carcinoma in a non-smoking patient and has been confirmed to have the same phenotype of the original tumor biopsy. Heterotransplantation and cytogenetic studies demonstrated its oncogenic derivation and monoclonality.[14] The human histone H_2B gene was fused with GFP and was transfected into human USC-HN3 cells to generate a stable line constitutively expressing GFP. The GFP fusion protein was incorporated into nucleosomes without affecting the cell-cycle progression.

Flow cytometry analysis

USC-HN3-GFP cells were selected by using FACS and the pure USC-HN3-GFP cells were isolated and grown in DMEM medium containing 10% FBS.

Injection of USC-HN3-GFP cells into the tongue of mice

Around 2.5 million stably transfected USC-HN3-GFP cells were injected into the tongues of normal SCID/nude mice. The injection of USC-HN3-GFP cells started development of tumors of the tongue after 6–8 days. At day 28, the mice were killed, and images of the tongue and the tumor tissue were captured using bright light and fluorescent microscopy. All care and treatment of animals was overseen by University of Southern California Institutional Animal Care and Use Committee. This committee oversees University of Southern California's animal programs, animal facilities and policies ensuring appropriate care, ethical use and humane treatment of animals.

Development of immortal cell line from migrated USC-HN3-GFP cells from the LN of mice

Skin and muscle were removed from the neck, and green-fluorescing cells were identified, which had migrated from the tongue as a primary tumor to the neck. Fluorescent microscopy was used to identify metastatic GFP-migrated tumor cells in the LNs. Metastatic tumor cells from the LN containing fluorescent tumor were harvested. From the metastatic tumor identified in the LN of the neck, we have developed the USC-HN3-GFP-G1 cell line. After development of the immortal cell line, the USC-HN3-GFP-G1 cells were reinjected into the tongues of mice and then again isolated and developed from the migrated cells from the LN of the neck. The isolated immortal cells were expanded to produce the USC-HN3-GFP-G2 cell line.

Total RNA extraction and analysis of global gene expression

Total RNA from these cell lines were isolated using Aurum Total RNA kit from Bio-Rad Laboratories, Inc., Hercules, CA, USA following the manufacturer's recommendations. Gene expression profiling was performed using the BeadChip HumanHT-12 v4 Expression kit from Illumina, which contains 47 231 gene probes (Illumina Inc., San Diego, CA, USA). The raw signal intensities were imported and analyzed using the GenomeStudio data analysis software (San Diego, CA, USA). Data were background subtracted, and the normalized signal intensities were exported to the Partek genomics expression analysis suite using the 'Partek's Report Plug-in' option in the GenomeStudio software (Partek, St Louis, MO, USA). Differentially expressed genes in the dox- or vehicle-treated samples were identified using the 'gene expression' workflow in the Partek software. The differentially expressed probes were further investigated using the Ingenuity Pathways Analysis package (IPA; http://www.ingenuity.com) to identify the association of differentially expressed genes within the 'cell growth and proliferation', 'tumor morphology', 'cellular development', 'cell death and survival', 'cell movement' and 'cell morphology' categories. Right-tailed Fisher's exact test as implemented in the IPA software was used to calculate a *P*-value for the probability of each network to be enriched by chance alone. Gene expression networks were analyzed for *ALDH1A3*, *OCT-4*, *CAV-1*, *TLR-4*, *MMP-7* and *TRIM-29*. The USC-HN3-GFP and USC-HN3-GFP-G2 cell line gene expression data were overlaid to visualize expression changes within those networks. The data discussed in this publication have been deposited in NCBI's Gene Expression Omnibus and are accessible through GEO Series accession number GSE41893 (http://www.ncbi.nlm.nih.gov/geo/query/acc.cgi?acc=GSE41893).

Western blot

For western blots, 50 μg of protein from the whole-cell lysates were fractionated in a 10% Tris-glycine polyacrylamide gel, electrotransferred to PVDF (polyvinylidene difluoride) membranes, and probed overnight with primary antibody for activated CAV-1, TLR-4, MMP-7, E-Cadherin, ALDH1A3, OCT-4 and TRIM-29. Blots were stripped and reprobed for GAPDH (glyceraldehyde 3-phosphate dehydrogenase; clone FL-335; Santa Cruz Biotechnology), to normalize the amount of sample loaded. Horseradish peroxidase-conjugated secondary antibodies (Caltag, Burlingame, CA, USA) were then applied, followed by signal detection using Immobilon Western Chemiluminescent HRP Substrate (Millipore, Billerica, MA, USA).

IHC

For IHC studies, cells and tissue sections from USC-HN3-GFP-G1 and USC-HN3-GFP-G2 tumors grown in SCID/nude mice were used and compared with stained, fixed slides of the original tumor. USC-HN1-GFP-G1 and USC-HN1-GFP-G2 cells grown for 24 h directly on sterile printed $25 \times 75\ mm^2$ glass slides (Bellco Glass, Inc., Vineland, NJ, USA) were fixed sequentially with 2% parafolmaldehyde (Polysciences, Inc., Warrington, PA, USA) for 10 min at room temperature and acetone for 5 min at $-20\ ^{\circ}C$. For tissue sections, excised heterotransplanted USC-HN3-GFP-G1 and USC-HN3-GFP-G2 tumors from SCID/nude mice were fixed overnight in 10% neutral-buffered formalin and embedded in paraffin blocks. For cell culture and tissue morphology studies, Wright–Giemsa and hematoxylin and eosin stains were used, respectively, on air-dried cell preparations. In addition, USC-HN3-GFP-G1 and USC-HN3-GFP-G2 cell preparations and 5-micron tissue sections were stained with monoclonal antibodies against human ALDH1A3, TRIM-29, MMP-7, CAV-1, E-Cadherin and OCT-4. Observation, evaluation and image acquisition were made using Leica DM2500 microscope (Leica Microsystems, Buffalo Grove, IL, USA) connected to an automated, digital SPOT RTke camera and SPOT Advanced Software (SPOT Diagnostic Instrument Inc., Sterling Heights, MI USA). Images were further resized and brightened for publication using the Adobe Photoshop software (Adobe, San Jose, CA, USA). The same procedure was carried out for patient tissue sections with the following antibodies: TRIM-29, ALDH1A3, CAV-1, MMP-7 and β-catenin.

CONFLICT OF INTEREST

The authors declare no conflict of interest.

ACKNOWLEDGEMENTS

We thank Susan McDonald for her help in the patients' chart. We also thank Raj Dedhia and Farshad Chowdhury for doing the chart review of all the patients and proofreading the manuscript. This work was supported by the generous grants from the Health Research Association and RAM capital. RM had complete access to the data used in this manuscript and is without any conflict of interest. Dr Baniwal was supported from the Zumberge foundation.

REFERENCES

1 Parkin DM, Bray F, Ferlay J, Pisani P. Global cancer statistics, 2002. *CA Cancer J Clin* 2005; **55**: 74–108.
2 Hecht SS. Tobacco carcinogens, their biomarkers and tobacco-induced cancer. *Nat Rev Cancer* 2003; **3**: 733–744.
3 Agrawal N, Frederick MJ, Pickering CR, Bettegowda C, Chang K, Li RJ *et al.* Exome sequencing of head and neck squamous cell carcinoma reveals inactivating mutations in NOTCH1. *Science (New York, NY)* 2011; **333**: 1154–1157.
4 Stransky N, Egloff AM, Tward AD, Kostic AD, Cibulskis K, Sivachenko A *et al.* The mutational landscape of head and neck squamous cell carcinoma. *Science (New York, NY)* 2011; **333**: 1157–1160.
5 Licitra L, Perrone F, Bossi P, Suardi S, Mariani L, Artusi R *et al.* High-risk human papillomavirus affects prognosis in patients with surgically treated oropharyngeal squamous cell carcinoma. *J Clin Oncol* 2006; **24**: 5630–5636.
6 Zhang X, Su L, Pirani AA, Wu H, Zhang H, Shin DM *et al.* Understanding metastatic SCCHN cells from unique genotypes to phenotypes with the aid of an animal model and DNA microarray analysis. *Clin Exp Metastasis* 2006; **23**: 209–222.
7 Vermorken JB, Herbst RS, Leon X, Amellal N, Baselga J. Overview of the efficacy of cetuximab in recurrent and/or metastatic squamous cell carcinoma of the head and neck in patients who previously failed platinum-based therapies. *Cancer* 2008; **112**: 2710–2719.

8 Kalluri R, Neilson EG. Epithelial-mesenchymal transition and its implications for fibrosis. *J Clin Invest* 2003; **112**: 1776–1784.
9 Zuo JH, Zhu W, Li MY, Li XH, Yi H, Zeng GQ *et al.* Activation of EGFR promotes squamous carcinoma SCC10A cell migration and invasion via inducing EMT-like phenotype change and MMP-9-mediated degradation of E-cadherin. *J Cell Biochem* 2011; **112**: 2508–2517.
10 Zhang Z, Filho MS, Nor JE. The biology of head and neck cancer stem cells. *Oral Oncol* 2012; **48**: 1–9.
11 Chute JP, Muramoto GG, Whitesides J, Colvin M, Safi R, Chao NJ *et al.* Inhibition of aldehyde dehydrogenase and retinoid signaling induces the expansion of human hematopoietic stem cells. *Proc Natl Acad Sci USA* 2006; **103**: 11707–11712.
12 Sano D, Myers JN. Xenograft models of head and neck cancers. *Head Neck Oncol* 2009; **1**: 32.
13 Yigitbasi OG, Younes MN, Doan D, Jasser SA, Schiff BA, Bucana CD *et al.* Tumor cell and endothelial cell therapy of oral cancer by dual tyrosine kinase receptor blockade. *Cancer Res* 2004; **64**: 7977–7984.
14 Liebertz DJ, Lechner MG, Masood R, Sinha UK, Han J, Puri RK *et al.* Establishment and characterization of a novel head and neck squamous cell carcinoma cell line USC-HN1. *Head Neck Oncol* 2010; **2**: 5.
15 Goldberg HI, Lockwood SA, Wyatt SW, Crossett LS. Trends and differentials in mortality from cancers of the oral cavity and pharynx in the United States, 1973-1987. *Cancer* 1994; **74**: 565–572.
16 Zhang X, Liu Y, Gilcrease MZ, Yuan XH, Clayman GL, Adler-Storthz K *et al.* A lymph node metastatic mouse model reveals alterations of metastasis-related gene expression in metastatic human oral carcinoma sublines selected from a poorly metastatic parental cell line. *Cancer* 2002; **95**: 1663–1672.
17 Rosano L, Cianfrocca R, Spinella F, Di Castro V, Nicotra MR, Lucidi A *et al.* Acquisition of chemoresistance and EMT phenotype is linked with activation of the endothelin A receptor pathway in ovarian carcinoma cells. *Clin Cancer Res* 2011; **17**: 2350–2360.
18 Siu A, Lee C, Dang D, Lee C, Ramos DM. Stem cell markers as predictors of oral cancer invasion. *Anticancer Res* 2012; **32**: 1163–1166.
19 Lo WL, Chien Y, Chiou GY, Tseng LM, Hsu HS, Chang YL *et al.* Nuclear localization signal-enhanced RNA interference of EZH2 and Oct4 in the eradication of head and neck squamous cell carcinoma-derived cancer stem cells. *Biomaterials* 2012; **33**: 3693–3709.
20 Marcato P, Dean CA, Giacomantonio CA, Lee PW. Aldehyde dehydrogenase: its role as a cancer stem cell marker comes down to the specific isoform. *Cell Cycle (Georgetown, Tex)* 2011; **10**: 1378–1384.
21 Luo Y, Dallaglio K, Chen Y, Robinson WA, Robinson SE, McCarter MD *et al.* ALDH1A isozymes are markers of human melanoma stem cells and potential therapeutic targets. *Stem cells (Dayton, Ohio)* 2012; **30**: 2100–2113.
22 Wang L, Heidt DG, Lee CJ, Yang H, Logsdon CD, Zhang L *et al.* Oncogenic function of ATDC in pancreatic cancer through Wnt pathway activation and beta-catenin stabilization. *Cancer Cell* 2009; **15**: 207–219.
23 Zhou ZY, Yang GY, Zhou J, Yu MH. Significance of TRIM29 and beta-catenin expression in non-small-cell lung cancer. *J Chin Med Assoc* 2012; **75**: 269–274.
24 Hung KF, Lin SC, Liu CJ, Chang CS, Chang KW, Kao SY. The biphasic differential expression of the cellular membrane protein, caveolin-1, in oral carcinogenesis. *J Oral Pathol Med* 2003; **32**: 461–467.
25 Xue J, Chen H, Diao L, Chen X, Xia D. Expression of caveolin-1 in tongue squamous cell carcinoma by quantum dots. *Eur J Histochem* 2010; **54**: e20.
26 Zhao X, Ma C, Cai X, Lei D, Liu D, Xu F *et al.* RNA interference of caveolin-1 via lentiviral vector inhibits growth of hypopharyngeal squamous cell carcinoma FaDu cells *In Vitro* and *In Vivo*. *Asian Pac J Cancer Prev* 2011; **12**: 397–401.
27 Lu Z, Ghosh S, Wang Z, Hunter T. Downregulation of caveolin-1 function by EGF leads to the loss of E-cadherin, increased transcriptional activity of beta-catenin, and enhanced tumor cell invasion. *Cancer Cell* 2003; **4**: 499–515.
28 Walton KA, Cole AL, Yeh M, Subbanagounder G, Krutzik SR, Modlin RL *et al.* Specific phospholipid oxidation products inhibit ligand activation of toll-like receptors 4 and 2. *Arterioscler Thromb Vasc Biol* 2003; **23**: 1197–1203.
29 Szczepanski MJ, Czystowska M, Szajnik M, Harasymczuk M, Boyiadzis M, Kruk-Zagajewska A *et al.* Triggering of Toll-like receptor 4 expressed on human head and neck squamous cell carcinoma promotes tumor development and protects the tumor from immune attack. *Cancer Res.* 2009; **69**: 3105–3113.
30 Jing YY, Han ZP, Sun K, Zhang SS, Hou J, Liu Y *et al.* Toll-like receptor 4 signaling promotes epithelial-mesenchymal transition in human hepatocellular carcinoma induced by lipopolysaccharide. *BMC Med* 2012; **10**: 98.
31 Machida K, Chen CL, Liu JC, Kashiwabara C, Feldman D, French SW *et al.* Cancer stem cells generated by alcohol, diabetes, and hepatitis C virus. *J Gastroenterol Hepatol* 2012; **27**(Suppl 2): 19–22.
32 Chang CJ, Chien Y, Lu KH, Chang SC, Chou YC, Huang CS *et al.* Oct4-related cytokine effects regulate tumorigenic properties of colorectal cancer cells. *Biochem Biophys Res Commun* 2011; **415**: 245–251.
33 Hwang WL, Yang MH, Tsai ML, Lan HY, Su SH, Chang SC *et al.* SNAIL regulates interleukin-8 expression, stem cell-like activity, and tumorigenicity of human colorectal carcinoma cells. *Gastroenterology* 2011; **141**: 279–291.
34 Wang WS, Chen PM, Wang HS, Liang WY, Su Y. Matrix metalloproteinase-7 increases resistance to Fas-mediated apoptosis and is a poor prognostic factor of patients with colorectal carcinoma. *Carcinogenesis* 2006; **27**: 1113–1120.
35 Ii M, Yamamoto H, Adachi Y, Maruyama Y, Shinomura Y. Role of matrix metalloproteinase-7 (matrilysin) in human cancer invasion, apoptosis, growth, and angiogenesis. *Exp Biol Med* 2006; **231**: 20–27.
36 Shibata S, Marushima H, Asakura T, Matsuura T, Eda H, Aoki K *et al.* Three-dimensional culture using a radial flow bioreactor induces matrix metalloprotease 7-mediated EMT-like process in tumor cells via TGFbeta1/Smad pathway. *Int J Oncol* 2009; **34**: 1433–1448.